High CMRR and Wideband Current-Mode Instrumentation Amplifier Using Fully Differential Operational Floating Conveyor

Hossam ElGemmazy[1], Amr Helmy[2], Hassan Mostafa[2,3], Yehea Ismail[1,2]

[1]*Department of Electronics and Communications Engineering, The American University in Cairo, Egypt*
[2]Center of Nanoelectronics and Devices (CND) at Zewail City of Science and Technology/AUC, Cairo, Egypt
[3]*Department of Electronics and Communications Engineering, Cairo University, Giza, Egypt*
hossamm, anhelmy, hmoustafa, y.ismail@aucegypt.edu

***Abstract*—This paper presents a current-mode instrumentation amplifier (CMIA) based on the fully differential operational floating conveyor (FD-OFC). The FD-OFC, as a novel general purpose building block introduced by the authors, has the advantages of fully differential signal processing like higher design flexibility and higher noise rejection. The proposed CMIA provides wide bandwidth reaches 975 MHz and high CMRR exceeds 240 dB. The simplicity of the design is one of its advantages where only one FD-OFC is required and it can operate under biasing condition as low as 1.2 Volt. The operating conditions recommend the proposed CMIA to be integrated to wide range of low power high speed application, particularly when a high CMRR is required. The terminal behavior of the proposed design is mathematically modeled and its operation is simulated using the UMC 130 nm technology kit in Cadence environment.**

Keywords—Current-mode circuits; Current conveyors; Instrumentation amplifier; Fully differential operational floating conveyor (FD-OFC); Common mode rejection ratio (CMRR).

I. Introduction

Instrumentation amplifiers are widely used in many application areas, such as medical instrumentation [1], sensor readout integrated circuits [2] and data acquisition [3]. These amplifiers are mainly employed to amplify weak differential signals and omit unwanted common-mode signals. Therefore, the common mode rejection ratio (CMRR) is a key parameter to measure the quality of an instrumentation amplifier. Many techniques are used to implement the instrumentation amplifiers using voltage-mode devices like Operational Amplifiers (Op-Amp) and/or current-mode devices like second generation Current Conveyors (CCII). The gain bandwidth product (GBP) is fixed for voltage-mode circuits while it's not fixed for current-mode circuits [3]. The fixed GBP means that the bandwidth is highly dependent on the gain which induces a trade-off between these two quantities. Due to this gain-bandwidth dependency of the voltage-mode instrumentation amplifiers (VMIA), the bandwidth is usually narrow at high differential gain and CMRR. Moreover, the high CMRR requires accurate matching of the external components. On the other hand, current-mode instrumentation amplifiers (CMIA) don't suffer from these drawbacks where they can realize wide bandwidth with high CMRR and differential gains independently on the external component matching.

The CCII as a current-mode device was first introduced in [4] as three terminal device. Fig. 1 (a) and (b) illustrate typical block diagram representation for the non-inverting and the inverting versions of the second generation current conveyor (CCII+/-).

The principle of operation of the CCII+ can be described as follows: The voltage applied at terminal Y exactly appears at X with zero current at terminal Y (i.e., infinite input impedance at terminal Y) and independent voltage and current at terminal X of Vx and Io respectively. The voltage following action at the input ports is accompanied by conveying the current Io to the output terminal Z. This mechanism of operation can be represented using the following matrix form as:

$$\begin{bmatrix} I_Y \\ V_X \\ I_Z \end{bmatrix} = \begin{bmatrix} 0 & 0 & 0 \\ 1 & 0 & 0 \\ 0 & \pm 1 & 0 \end{bmatrix} \begin{bmatrix} V_Y \\ I_X \\ V_Z \end{bmatrix} \qquad (1)$$

(where the + and – signs correspond to the CCII+ and the CCII- respectively)

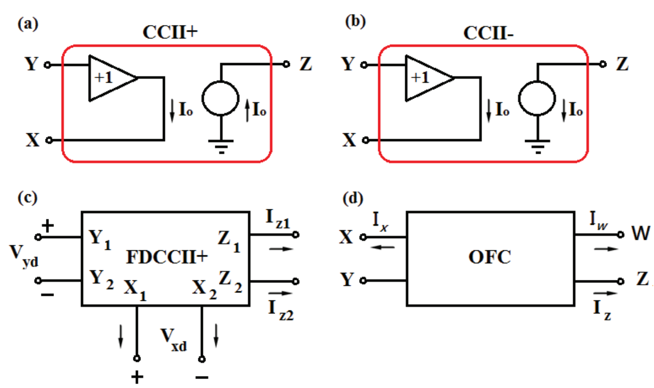

Fig. 1. Block diagram representation of (a): non-inverting second generation current conveyor, (b): inverting second generation current conveyor, (c): fully differential current conveyor and (d): operational floating conveyor.

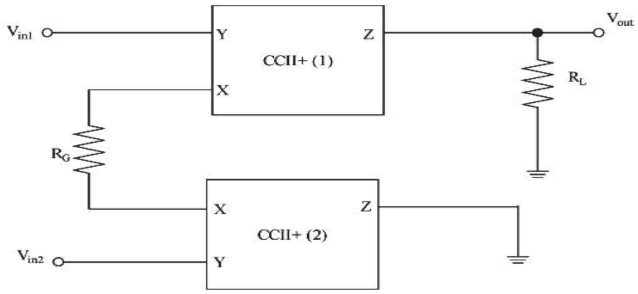

Fig. 2: CMIA using two CCII+ [10]

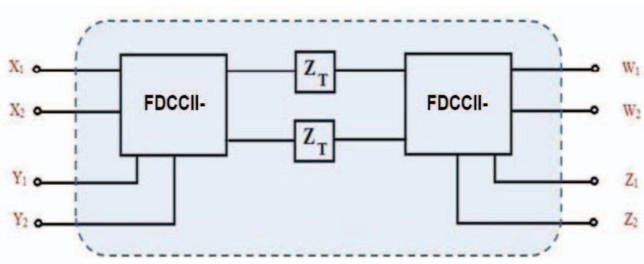

Fig. 3: Block diagram representation of the FD-OFC [7]

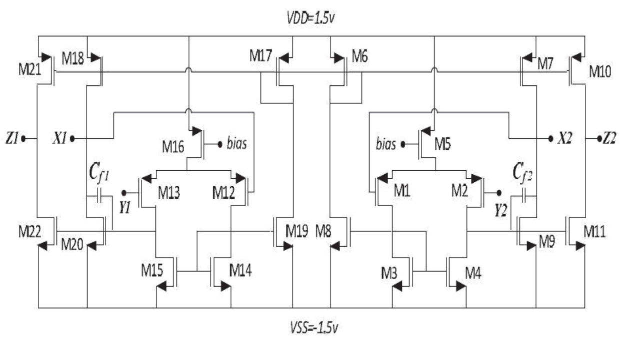

Fig. 4: Schematic diagram representation of the FDCCII- [18]

The Fully Differential Current Conveyor (FDCCII), as its name implied is the differential form of the CCII. The differential action is achieved by splitting each of the three terminals of the CCII into two terminals, such that the FDCCII has six terminals as shown in Fig. 1 (c) [5].

One of the CMIA implementations using the CCII [10] is shown in Fig. 2. The design contains also the gain setting resistance R_G and the load resistance R_L. Simplicity is the advantage of this design but the accuracy of the design is limited by the tolerance of terminal X equivalent input resistance R_X.

The differential mode gain $A_d(s)$ is given by:

$$A_d(S) = \frac{V_O}{V_{i1} - V_{i2}} = \frac{R_L}{R_G + 2R_X} \cdot \frac{1}{1 + SCR_L} \quad (2)$$

where C is the CCII+ equivalent output capacitance.

II. THE OPERATIONAL FLOATING CONVEYOR

The concept of the Operational Floating Conveyor (OFC), which offers more features than both the CCII and FDCCII, has been first introduced [6]. Fig. 1 (d) illustrates the operation of the OFC via its block diagram representation. As clear from this figure, the OFC is a four (2x2) terminal device. Ideally, the voltage applied at terminal Y appears exactly at the terminal X with Vx is invariant with the input current Ix. This is the voltage following action at the input ports. The current at terminal Y is ideally zero, corresponding to infinite input impedance at Y. The voltage at terminal W is the product of Ix and the trans-impedance gain Zt while Iw is ideally conveyed to the terminal Z as Iz. This action is called the current following action at the output ports. This ideal operation of the voltage and current actions can be mathematically represented in matrix form as:

$$\begin{bmatrix} V_X \\ I_Y \\ V_W \\ I_Z \end{bmatrix} = \begin{bmatrix} 0 & 1 & 0 & 0 \\ 0 & 0 & 0 & 0 \\ Zt & 0 & 0 & 0 \\ 0 & 0 & 1 & 0 \end{bmatrix} \begin{bmatrix} I_X \\ V_Y \\ I_W \\ V_Z \end{bmatrix} \quad (3)$$

III. THE FULLY DIFFERENTIAL OPERATIONAL FLOATING CONVEYOR

The Fully Differential Operational Floating Conveyor (FD-OFC) concept and designs are first introduced by the authors [7] as an extension of the conventional OFC. The FD-OFC has twice as much number as those in the OFC, resulting in the operation in the fully differential mode. Accordingly, the FD-OFC can be represented as an 8 (4x4) port general purpose analog building block as shown in Fig. 3. The schematic diagram of the FDCCII- is shown in Fig. 4. The terminal behavior can be expressed in terms of a transfer matrix of the FD-OFC "$T^{(FD-OFC)}$" as follows:

$$\begin{bmatrix} V_{xd} \\ I_{yd} \\ V_{wd} \\ I_{zd} \end{bmatrix} = T^{(FD-OFC)} \begin{bmatrix} I_{xd} \\ V_{yd} \\ I_{wd} \\ V_{zd} \end{bmatrix} \quad (4)$$

Where

$$\begin{aligned} I_{xd} &= \left[I_{x1} \quad I_{x2}\right]^T, \quad I_{yd} = \left[I_{y1} \quad I_{y2}\right]^T, \\ I_{wd} &= \left[I_{w1} \quad I_{w2}\right]^T, \quad I_{zd} = \left[I_{z1} \quad I_{z2}\right]^T, \\ V_{xd} &= \left[V_{x1} \quad V_{x2}\right]^T, \quad V_{yd} = \left[V_{y1} \quad V_{y2}\right]^T, \\ V_{wd} &= \left[V_{w1} \quad V_{w2}\right]^T, \quad V_{zd} = \left[V_{z1} \quad V_{z2}\right]^T \end{aligned} \quad (5)$$

And $[.]^T$ denotes the matrix transpose operator.

$$T^{(FD-OFC)} = \begin{bmatrix} 0 & 0 & 1 & 0 & 0 & 0 & 0 & 0 \\ 0 & 0 & 0 & 1 & 0 & 0 & 0 & 0 \\ 0 & 0 & 0 & 0 & 0 & 0 & 0 & 0 \\ 0 & 0 & 0 & 0 & 0 & 0 & 0 & 0 \\ Z_t & 0 & 0 & 0 & 0 & 0 & 0 & 0 \\ 0 & Z_t & 0 & 0 & 0 & 0 & 0 & 0 \\ 0 & 0 & 0 & 0 & 1 & 0 & 0 & 0 \\ 0 & 0 & 0 & 0 & 0 & 1 & 0 & 0 \end{bmatrix} \quad (6)$$

IV. THE PROPOSED CMIA USING FD-OFC

Fig. 5 depicts the proposed CMIA using one Fully Differential Operational Floating Conveyor (FD-OFC). The design contains also the gain setting resistance R_G and the load resistance R_L in addition to two feedback resistances (R_{W1} and R_{W2}). These feedback resistances allows the FD-OFC to operate as CCII+ while simultaneously reduces the input resistance of port X similar to the conventional OFC [8]. This design is more accurate than Fig. 2 design because it's independent on terminal X input resistance R_X and depends only on the external resistances R_G and R_L. Furthermore, it uses only one building block (FD-OFC) and provides higher bandwidth and CMRR compared to the other designs [10-17].

The ideal differential mode gain $A_d(s)$ can be derived as follows:

$$I_X = \frac{V_{X1} - V_{X2}}{R_G} = \frac{V_{in1} - V_{in2}}{R_G} \quad (7)$$

$$I_L = I_X \quad (8)$$

$$V_O = I_X \left(R_L \,//\, \frac{1}{SC_Z} \right) \quad (9)$$

where C_Z is the equivalent output capacitance.

$$V_O = \frac{(V_{in1} - V_{in2})}{R_G} \left(R_L \,//\, \frac{1}{SC_Z} \right) \quad (10)$$

$$V_O = \frac{(V_{in1} - V_{in2})}{R_G} \left(\frac{R_L}{1 + SC_Z R_L} \right) \quad (11)$$

The differential mode gain $A_d(s)$ is given by:

$$A_d(S) = \frac{V_O}{V_{in1} - V_{in2}} = \frac{R_L}{R_G \left(1 + SC_Z R_L\right)} \quad (12)$$

It is clear from (12) that the ratio R_L/R_G controls the differential gain while the bandwidth is set using $C_Z R_L$. This means that the differential gain can be controlled by R_G without affecting the bandwidth.

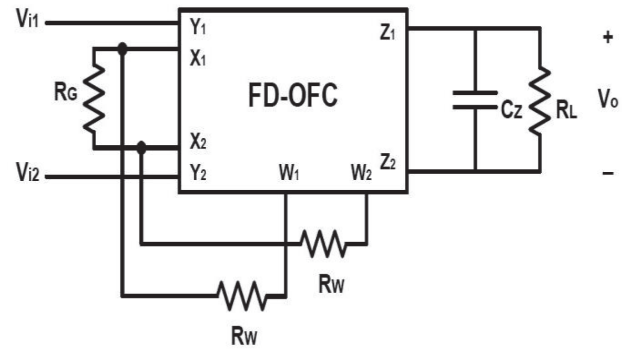

Fig. 5: The proposed CMIA using one FD-OFC

V. SIMULATION RESULTS

The proposed CMIA circuit is simulated using UMC 130 nm CMOS-based technology kit in Cadence environment. The entire circuit is simulated using the same transistor specification of the FD-OFC [7] and 1.2 Volt biasing conditions. The frequency response of different differential gains of the circuit are shown in Fig. 6 using R_W = 0.25 KΩ, R_L = 1 KΩ and R_G = 10 Ω, 20 Ω, 50 Ω and 100 Ω. The actual differential gain is much closer to the ideal gain for smaller gain values. These different gain values are invariant for AC signals having frequencies up to about 100 MHz. The differential gain bandwidth is approximately gain-independent (it varies between 630 MHz and 975 MHz for the shown differential gain values). The calculated average power dissipation for the design is 19.7 mWatt. The Common Mode Rejection Ratio (CMRR) is measured for the proposed CMIA for the different differential gain values [9]. Fig. 7 displays the CMRR for the proposed CMIA for R_G = 50 Ω. As expected, using the FD-OFC as a fully differential building block led to a very high CMRR.

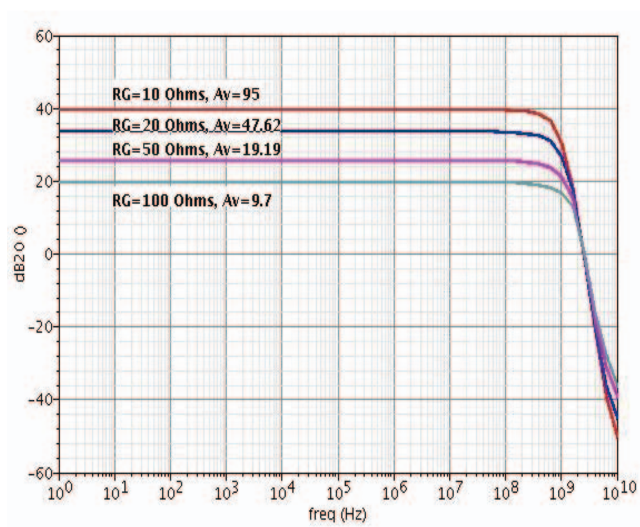

Fig. 6: Differential gain frequency response of the proposed CMIA

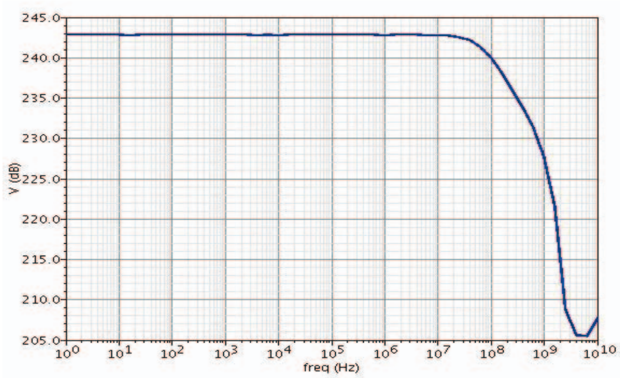

Fig. 7: CMRR frequency response for the proposed CMIA for R_G = 50 Ω.

The proposed CMIA exhibits wider bandwidth compared to other designs, higher CMRR and uses only one building block (FD-OFC). Based on the simulation results, Table 1 shows a comparison between the proposed CMIA and other conveyor designs [15,17].

TABLE I. COMAPRISON BETWEEN DIFFERENT DESIGNS

Ref. No.	Diff. Gain (dB)	Diff. Gain -3dB Freq.	CMRR (dB)	CMRR -3dB Freq.	Building Blocks
[10]	20, 26, 29.54, 32	1.2-2.3 MHz	100	NA	2 CCII+
[11]	40, 25, 5.7	1.44 MHz	95	65 KHz	3 CCII+
[12]	29, 24, 19	591.6 KHz	95	2 KHz	2 CCII+
[13]	40, 20, 0	1.5-2.97 KHz	55	10 KHz	2 CCII+, 2 Op-Amp
[14]	14, 19.6, 25	10 MHz	147	35 KHz	3 CCCII
[15]	32, 26, 12, 6	1.2 MHz	76	185 KHz	2 OFCC
[16]	16.7, 21, 25.4, 28.7	70.1 MHz	142	NA	2 CCCII
[17] Top. 3	21, 25, 31, 36	20.85 MHz	55	349 KHz	3 OFCC
[17] Top. 7	23, 17, 11, 9	30 MHz	85	32 KHz	4 OFCC
This work	39.55, 33.6, 25.7, 19.74	630- 975 MHz	243	104 MHz	1 FD-OFC

VI. CONCLUSION

A novel current-mode instrumentation amplifier (CMIA) is proposed using one FD-OFC as a fully differential building block. The proposed design is simple and can operate under biasing condition as low as 1.2 Volt. It also provides wider bandwidth and higher CMRR (even at high frequencies) compared to other instrumentation amplifiers. The bandwidth is approximately gain-independent and the high CMRR doesn't require external component matching. The performance of the proposed CMIA is verified via simulation using UMC 130 nm technology in Cadence environment. The simulation results indicate that the proposed design is perfectly suitable for low power high speed application, particularly when a high CMRR is required.

ACKNOWLEDGMENT

The authors would like to thank the supporting and funding agencies. This work was supported in part by Cairo University, the Zewail City of Science and Technology, in part by AUC, in part by the STDF, in part by Intel, in part by Mentor Graphics, in part by ITIDA, in part by SRC, in part by ASRT, in part by NTRA, and in part by MCIT.

REFERENCES

[1] Pallas-Areny, R., Webster, J.G.: 'AC instrumentation amplifier for bioimpedance measurements', IEEE Trans. Biomed. Eng., 1993, 40, (8), pp. 830–833

[2] Wu, R., Huijsing, J.H., Makinwa, K.A.A.: 'Precision instrumentation amplifiers and read-out integrated circuits' (Springer, 2013)

[3] C. Toumazou, F. J. Lidgey, and D. Haigh, Analog IC design: the current-mode approach, vol. 2. Presbyterian Publishing Corp, 1990.

[4] A.S. Sedra, and K.C. Smith, A second-generation current conveyor and its applications, IEEE Transactions on Circuit Theory, CT-17, pp.132-134, 1970.

[5] Soliman A. Mahmoud, Eman A. Soliman, Maurits Ortmanns, Ahmed M. Soliman, "High speed fully differential second generation current conveyor", Circuits and Systems (MWSCAS) 2010 53rd IEEE International Midwest Symposium on, pp. 953-956, 2010, ISSN 1548-3746.

[6] C. Toumazou, A. Payne and F. Lidgey, Operational floating conveyor, Electron. Lett. 27 (1991) 651–652.

[7] Elgemmazy, H., A. Helmy, H. Mostafa, and Y. Ismail, "A Novel CMOS-based Fully Differential Operational Floating Conveyor", IEEE International Symposium on Very Large Scale Integration (ISVLSI 2017), Bochum-Germany, pp. 604-608, 2017.

[8] Hassan M. Hassan and Ahmed M. Soliman, Novel CMOS realizations of the operational floating conveyor and applications, Journal of Circuits, Systems and Computers, vol. 14, no. 6, pp. 11131143, July 2005.

[9] R. P. Areny and J. G. Webster, "Common mode rejection ratio in differential amplifiers," Instrumentation and Measurement, IEEE Transactions on, vol. 40, no. 4, pp. 669–676, 1991.

[10] B. Wilson, "Universal conveyor instrumentation amplifier," Electronics letters, vol. 25, no. 7, pp. 470–471, 1989.

[11] A. Khan, M. Al-Turaigi, M. Ei-Ela, and others, "An improved current-mode instrumentation amplifier with bandwidth independent of gain," Instrumentation and Measurement, IEEE Transactions on, vol. 44, no. 4, pp. 887–891, 1995.

[12] S. J. Azhari and H. Fazlalipoor, "A novel current mode instrumentation amplifier (CMIA) topology," Instrumentation and Measurement, IEEE Transactions on, vol. 49, no. 6, pp. 1272–1277, 2000.

[13] Gift, S.J.G.: 'An enhanced current mode instrumentation amplifier', IEEE Trans. Instrumentation and Measurement, 2001, 50, (1), pp. 85–88

[14] Maheshwari, S.: 'High CMRR wide bandwidth instrumentation amplifier using current controlled conveyors', Int. J. Electron., 2002, 89, (12), pp. 889–896

[15] Yehia H. Ghallab, W. Badawy, K. V. I. S. Kaler, and B. J. Maundy, "A novel current-mode instrumentation amplifier based on operational floating current conveyor," IEEE Transactions on Instrumentation and Measurement, vol. 54, no. 5, pp. 1941–1949, 2005.

[16] Ercan, H., Tekin, S.A., Alci, M.: 'Voltage and current controlled high CMRR instrumentation amplifier using CMOS current conveyors', Turk J. Electr. Eng. Comp. Sci., 2012, 20, (4), pp. 547–556

[17] Pandey, N., Nand, D., Pandey, R. Generalised operational floating current conveyor based instrumentation amplifier. IET Circuits Devices Syst., 10(3), 209−219, 2016.

[18] I. G. Finvers, B. J. Maundy, I. A. Omole and P. Aronhime, On the design of CMOS current conveyors, Can. J. Elect. Comput. Eng. 26 (2001) 15–21